



Published in final edited form as:

Curr Biol. 2008 June 3; 18(11): 808–813. doi:10.1016/j.cub.2008.04.050.

CED-10/Rac1 mediates axon guidance by regulating the asymmetric distribution of MIG-10/lamellipodin

Christopher C. Quinn^{1,*}, Douglas S. Pfeil¹, and William G. Wadsworth^{1,*}

¹ Department of Pathology, Robert Wood Johnson Medical School, Piscataway, NJ

Abstract

Axon migrations are guided by extracellular cues that induce asymmetric outgrowth activity in the growth cone [1,2]. Several intracellular signaling proteins have been implicated in the guidance response [3–10]. However, how these proteins interact to generate asymmetric outgrowth activity is unknown. Here, we present evidence that in *C. elegans*, the CED-10/Rac1 GTPase binds to and causes asymmetric localization of MIG-10/lamellipodin, a protein that regulates actin polymerization and has outgrowth-promoting activity in neurons[5,11]. Genetic analysis indicates that *mig-10* and *ced-10* function together to orient axon outgrowth. The RAPH domain of MIG-10 binds to activated CED-10/Rac1 and *ced-10* function is required for the asymmetric localization of MIG-10 that occurs in response to the UNC-6/netrin guidance cue. We also show that asymmetric localization of MIG-10 in growth cones is associated with asymmetric concentrations of f-actin and microtubules. These results suggest that CED-10/Rac1 is asymmetrically activated in response to the UNC-6/netrin signal, thereby causing asymmetric recruitment of MIG-10/lamellipodin. We propose that the interaction between activated CED-10/Rac1 and MIG-10/lamellipodin triggers local cytoskeletal assembly and polarizes outgrowth activity in response to UNC-6/netrin.

Results and Discussion

Activated CED-10/Rac1 binds to MIG-10/lamellipodin

CED-10/Rac1 is a small GTPase that has been implicated in axon guidance [4,12,13]. Guidance cues stimulate guanine nucleotide exchange factors (GEFs) to cause activation of Rac [3,14]. However, the events that act downstream of Rac activation to mediate the guidance response are not well understood. In particular, it is not clear how activation of Rac leads to asymmetric outgrowth.

To address this question, we considered MIG-10/lamellipodin as a potential effector of CED-10/Rac-1 during the guidance response. Both MIG-10/lamellipodin and CED-10/Rac1 have been implicated in UNC-6/netrin signaling [5,7,8,11]. Genetic analysis in *C. elegans* has demonstrated that CED-10 functions downstream of the UNC-40/DCC receptor and that it mediates the guidance response to the UNC-6/netrin guidance cue [8]. MIG-10 has also been implicated in UNC-6 signaling and includes a Ras Association (RA) domain whose binding partner has not been identified [5]. Therefore, we asked if MIG-10/lamellipodin can bind to

*To whom correspondence should be addressed at: Department of Pathology, Robert Wood Johnson Medical School, 675 Hoes Lane, Piscataway, NJ 08854-5653, E-mail: quinncc@umdnj.edu, Phone: (732) 235-4849, Fax: (732) 235-4825, E-mail: william.wadsworth@umdnj.edu, Phone: (732) 235-5768, Fax: (732) 235-4825.

Publisher's Disclaimer: This is a PDF file of an unedited manuscript that has been accepted for publication. As a service to our customers we are providing this early version of the manuscript. The manuscript will undergo copyediting, typesetting, and review of the resulting proof before it is published in its final citable form. Please note that during the production process errors may be discovered which could affect the content, and all legal disclaimers that apply to the journal pertain.

Rac or other members of the Rho family. We conducted *in vitro* binding assays using constitutively active Rho proteins (RhoL63, RacL61, and Cdc42L61). Since the *C. elegans* Rho proteins exhibit 90–97% similarity to their human homologs, we used the human homologs for binding assays. Rho family::GST fusion proteins were coupled to glutathione sepharose and incubated with lysates made from cells expressing the Ras Association-Plekstrin Homology (RAPH) domain of MIG-10 fused to GFP (MIG-10 RAPH::GFP). The MIG-10 RAPH::GFP domain bound to RacL61, but not to RhoL63 or Cdc42L61 (Figure 1A). Similar binding was observed with full length MIG-10::GFP (Figure S1A). To determine if binding between MIG-10 and Rac is GTP-dependent, we tested for binding with RacN17, a constitutively inactive mutant of Rac. MIG-10 RAPH::GFP did not bind to RacN17 (Figure 1B), indicating that binding is GTP-dependent. Since previous results have indicated that RIAM can bind to Rap1 [15], we also tested for binding between MIG-10 and Rap1. However we did not find evidence for binding between MIG-10 and Rap1 (Figure S1B). We also tested the mammalian homologs of MIG-10 and found that the Rac-GTP binding function is conserved in lamellipodin but not RIAM (Figure S1C-D).

CED-10/Rac1 mediates asymmetric distribution of MIG-10/lamellipodin

The UNC-6/netrin guidance cue induces asymmetry in the HSN neuron. The sources of UNC-6 are located ventrally of the HSN (see Figure 1C), causing the leading edge to be ventrally oriented. MIG-10/lamellipodin accumulates at the ventral edge of the HSN in the L2–L3 stages [6]. Since MIG-10 binds to activated Rac and Rac is thought to be activated at the leading edge of migrating cells [16], we asked if CED-10/Rac1 is required for the asymmetric localization of MIG-10.

In L3 stage wildtype animals we observed substantial variation in the shape of the HSN cell body. However, MIG-10::YFP was enriched at the ventral edge of nearly all of the HSN cell bodies observed. Quantitative image analysis revealed that the average ventral enrichment was more than two fold in wildtype animals (Figures 1D and 1F). By contrast, no enrichment of the membrane marker myristolated-GFP was observed (Figure 1F), indicating that the ventral enrichment of MIG-10::YFP is not the result of general membrane asymmetry.

To disrupt *ced-10* function we used the *ced-10(n3246)* allele because it is a strong loss-of-function allele with a mutation in a glycine residue that is thought to be required for conformational change induced by GTP-binding [17,18]. Loss of *ced-10* function strongly reduced the average MIG-10::YFP ventral enrichment (Figures 1E and 1F). Loss of *ced-10* function had no effect on the distribution of myristolated-GFP (Figure 1F). These results indicate that CED-10 function is required for the asymmetric distribution of MIG-10/lamellipodin. Combined with the biochemical data indicating GTP-dependent binding between CED-10/Rac1 and MIG-10/lamellipodin, these data suggest that activated CED-10/Rac1 recruits MIG-10/lamellipodin to the ventral edge.

CED-10/Rac1 functions with MIG-10/lamellipodin to orient HSN axon growth

MIG-10 accumulates asymmetrically to the ventral edge of the HSN cell body during the L2 and L3 stages [6]. At the beginning of the L4 stage the HSN extends an axon ventrally. Since CED-10 can mediate the asymmetric localization of MIG-10, we asked if these proteins function together to orient HSN axon growth. For these experiments we used the *ced-10(n3246)* strong loss-of-function allele and the *mig-10(ct41)* null allele. In the wildtype background, nearly all of the HSN axons were ventrally oriented as they grew out of the cell body (Figures 2A and 2B), with guidance defects observed in only 7% of the HSN axons (Figure 2G). Loss of *mig-10* function resulted in axon guidance defects in 46% of HSN neurons (Figure 2G). In nearly all cases the axons reached the ventral nerve cord after making short migrations in the anterior or posterior directions (Figure 2C and 2D). These defects cannot be

explained as a secondary consequence to the cell migration defects that are also observed in *mig-10* mutants (see Table S1). Loss of *ced-10* function resulted in similar defects in 28% of HSN neurons (Figures 2E-2G). The *ced-10;mig-10* double mutant was not enhanced relative to the either single mutant, indicating that MIG-10 and CED-10 function together to orient HSN axon growth.

MIG-10 functions downstream of CED-10/Rac1

The ability of CED-10 to regulate MIG-10 localization suggests that MIG-10 may function downstream of CED-10. To test this hypothesis we conducted an epistasis test with an activated *ced-10* mutant transgene. For these experiments we utilized the PDE neuron because it is possible to express an activated form of CED-10 in this neuron [19]. The PDE neuron normally has two unbranched processes emanating from the cell body. Expression of the constitutively active *ced-10(G12V)* transgene causes branched processes and ectopic processes emanating from the PDE cell body [19]. We found that this *ced-10* gain-of-function phenotype is strongly suppressed by loss of *mig-10* function (Table S2). For example, 91% of the PDE neurons expressing *ced-10(G12V)* had ectopic processes emanating from the cell body. The *mig-10(ct41)* null allele reduced this phenotype to 13%, indicating that MIG-10 functions downstream of CED-10.

MIG-10 acts with PAK-1 and in parallel to MAX-2 to orient HSN axon growth

Like MIG-10/lamellipodin, members of the PAK family can function downstream of Rac and have been implicated in axon guidance [9,20]. In *C. elegans*, there are two neuronally expressed members of the PAK family, known as MAX-2 and PAK-1 [20]. To better understand the role of these Rac binding proteins in axon guidance, we have analyzed double mutants between *mig-10* and the genes encoding each of the two members of the PAK family.

To determine the relationship between MIG-10 and MAX-2 we constructed a *max-2(cy2); mig10(ct41)* double mutant. Loss of *max-2* function did not produce HSN guidance defects greater than those observed in the wildtype background (Figures 3A and 3E). However, loss of *max-2* function significantly enhanced the penetrance and severity of defects associated with loss of *mig-10* function (Figures 3B-C and 3E). For example, in *mig-10* mutants, many HSN axons exhibit mild defects, but nearly all axons eventually reached the ventral nerve cord (VNC). However, in *mig-10;max-2* double mutants the majority of HSN axons failed to reach the VNC. The defects seen in *mig-10;max-2* double mutants were similar to those observed in an *unc-6* null allele (Figures 3D and 3E). These data indicate that MIG-10 acts in parallel to MAX-2 to guide the HSN axon.

To determine the relationship between MIG-10 and PAK-1 we constructed a *mig-10(ct41); pak-1(ok448)* double mutant. Loss of *pak-1* function resulted in mild guidance defects that were partially penetrant (Figure 3E). In double *mig-10;pak-1* mutants, this phenotype was not enhanced relative to either single mutant. This data suggests that PAK-1 and MIG-10 function in a common pathway to guide the HSN axon.

CED-10 is required for polarization of MIG-10-dependent axon growth

Our previous results have suggested that UNC-6 and SLT-1 guidance cues can regulate the polarity of process outgrowth. The AVM neuron is normally monopolar, extending a single process from its cell body. Overexpression of MIG-10 in the absence of UNC-6 and SLT-1 results in a multipolar phenotype, with multiple processes growing out of each cell body. The multipolar outgrowth can be suppressed by either UNC-6 or SLT-1, suggesting that either guidance cue can polarize MIG-10/lamellipodin-dependent outgrowth [5].

Since CED-10 can mediate asymmetric localization of MIG-10, we asked if CED-10 is required for the polarization of the MIG-10 outgrowth-promoting activity in response to guidance cues. AVM neurons overexpressing MIG-10 in the wildtype background rarely exhibited the multipolar phenotype (Figures 4A and 4D). Loss of *ced-10* function resulted in a multipolar phenotype in 22% of AVM neurons overexpressing MIG-10, with each neuron extending a short ectopic process (Figures 4B and 4D). Loss of both *ced-10* and *slt-1* enhanced both the penetrance and severity of this phenotype (Figures 4C and 4D). A similar experiment with loss of *ced-10* and *unc-6* function was not possible due to a lethal phenotype associated with *ced-10* (*n3246*); *unc-6(ev400)*. Expression of GFP under the same promoter never resulted in multipolar outgrowth in the *wildtype*, *ced-10*, or *ced-10;slt-1* backgrounds (Figure 4D). These data suggest that CED-10 can polarize the MIG-10 outgrowth-promoting activity in response to SLT-1. Although we were unable to directly assess a similar role in UNC-6 signaling, previous work indicates that CED-10 is involved in UNC-6 signaling [8] and that UNC-6 can polarize MIG-10 outgrowth-promoting activity[5]. Together, these observations suggest that CED-10 might also polarize the MIG-10 outgrowth-promoting activity in response to UNC-6.

Asymmetric MIG-10 is associated with asymmetric cytoskeleton in the growth cone

Growth cone turning is preceded by asymmetric enrichment of f-actin and microtubules [21–24]. MIG-10/lamellipodin can regulate actin polymerization, suggesting that MIG-10 may mediate asymmetric cytoskeletal assembly in the growth cone. To investigate the relationship between MIG-10 and asymmetric cytoskeletal enrichment, we examined the localization of actin and microtubules in cultured cortical neurons transfected with MIG-10::GFP. A subset (6/50) of these growth cones exhibited asymmetric concentration of MIG-10::GFP (see methods). All growth cones with asymmetric concentrations of MIG-10::GFP (6/6) had corresponding asymmetric concentrations of f-actin (Figures 5A and 5B). Furthermore, we observed bundled microtubules converging on the point of MIG-10 concentration (Figure 5C and 5D). Consistent with these observations, quantitative image analysis revealed that asymmetric MIG-10 concentrations were correlated with asymmetric concentrations of f-actin and microtubules (Figure 5E). These data indicate that asymmetric concentration of MIG-10 is associated with localized enrichment of f-actin and microtubules in the growth cone.

Model for interaction of Rac and MIG-10/lamellipodin in axon guidance

Our data suggest a model whereby asymmetric activation of CED-10/Rac1 leads to asymmetric recruitment of MIG-10/lamellipodin (Figure S2). MIG-10/lamellipodin can promote actin polymerization and promote lamellipodial protrusion[11]. Therefore, asymmetric localization of MIG-10/lamellipodin can provide the asymmetric actin-based protrusive activity that is required for growth cone steering. Asymmetric activation of CED-10/Rac1 is likely a consequence of the asymmetric localization of UNC-40/DCC that occurs in response to UNC-6/netrin. Consistent with this idea, UNC-40/DCC binds to Dock180, a GEF that activates Rac [3]. Our data suggests that MIG-10/lamellipodin is an effector for Rac, spatially coupling Rac activation to cytoskeletal assembly.

Roles of MIG-10/lamellipodin and PAK family members in axon guidance

Our data indicates that MIG-10/lamellipodin and MAX-2, a member of the PAK family, act in parallel genetic pathways to mediate axon guidance. Consistent with this model, both MIG-10/lamellipodin and PAK family members control the formation of lamellipodia [5,15,25,26]. Previous studies indicate that MAX-2 acts independently of the Rac proteins to control axon guidance [20]. Together, these observations suggest a model where MIG-10 acts downstream of CED-10/Rac1 and that MAX-2 acts in a parallel pathway that is independent of CED-10/Rac-1.

Our data also indicates that PAK-1, another member of the PAK family, acts in the same genetic pathway as MIG-10. Members of the PAK family can act with PIX as an upstream activator of Rac [25,26]. Therefore, PAK-1 could be involved in the activation of CED-10, thus triggering the interaction between CED-10 and MIG-10. Alternatively, PAK-1 and MIG-10 might simultaneously bind to MIG-10 as co-effectors. The precise role of the PAK family proteins in axon guidance will be an area for future investigations.

Role for asymmetric protein localization in axon guidance

Asymmetric protein localization is thought to drive cellular polarization. Although asymmetric protein localization has been well characterized in epithelial cell polarity and asymmetric cell division [27,28], its role during growth cone guidance is only just emerging. Recent work has shown that MIG-10 is asymmetrically localized in response to UNC-6/netrin [6]. Here, we show that CED-10/Rac1 controls the asymmetric localization of MIG-10. Asymmetric localization of MIG-10 may lead to asymmetric f-actin assembly, thus contributing to the polarization of the growth cone.

The role of asymmetric protein localization in growth cone guidance is conceptually related to asymmetric protein localization during the establishment of other types of cellular polarity. For instance, during asymmetric cell division, polarity is established through the asymmetric localization of the Par3/Par6 complex, which is regulated by binding to activated Rac and Cdc42 [29,30]. This is similar to the role of Rac in regulating the asymmetric localization of MIG-10/lamellipodin during the guidance response. Future research will help elucidate the similarities and differences between asymmetric protein localization in each context.

Supplementary Material

Refer to Web version on PubMed Central for supplementary material.

Acknowledgments

We thank Cornelia Bargmann and Elizabeth Ryder for discussions relating to this work; Jonathan Chernoff, Richard Cerrione, and Yuji Kohara for DNA plasmids; Erik Lundquist, Cornelia Bargmann and the Caenorhabditis Genetics Center for strains. This work was supported by National Institute of Neurological Disorders and Stroke grants F32NS468402 (C.C.Q.) and R01NS033156 (W.G.W.) and a grant from the New Jersey Commission on Spinal Cord Research.

References

1. Van Vactor D. Axon guidance. *Curr Biol* 1999;9:R797–799. [PubMed: 10556099]
2. Tessier-Lavigne M, Goodman CS. The molecular biology of axon guidance. *Science* 1996;274:1123–1133. [PubMed: 8895455]
3. Li X, Gao X, Liu G, Xiong W, Wu J, Rao Y. Netrin signal transduction and the guanine nucleotide exchange factor DOCK180 in attractive signaling. *Nat Neurosci*. 2007
4. Lundquist EA, Reddien PW, Hartwig E, Horvitz HR, Bargmann CI. Three *C. elegans* Rac proteins and several alternative Rac regulators control axon guidance, cell migration and apoptotic cell phagocytosis. *Development* 2001;128:4475–4488. [PubMed: 11714673]
5. Quinn CC, Pfeil DS, Chen E, Stovall EL, Harden MV, Gavin MK, Forrester WC, Ryder EF, Soto MC, Wadsworth WG. UNC-6/netrin and SLT-1/slit guidance cues orient axon outgrowth mediated by MIG-10/RIAM/lamellipodin. *Curr Biol* 2006;16:845–853. [PubMed: 16563765]
6. Adler CE, Fetter RD, Bargmann CI. UNC-6/Netrin induces neuronal asymmetry and defines the site of axon formation. *Nat Neurosci* 2006;9:511–518. [PubMed: 16520734]
7. Chang C, Adler CE, Krause M, Clark SG, Gertler FB, Tessier-Lavigne M, Bargmann CI. MIG-10/lamellipodin and AGE-1/PI3K promote axon guidance and outgrowth in response to slit and netrin. *Curr Biol* 2006;16:854–862. [PubMed: 16618541]

8. Gitai Z, Yu TW, Lundquist EA, Tessier-Lavigne M, Bargmann CI. The netrin receptor UNC-40/DCC stimulates axon attraction and outgrowth through enabled and, in parallel, Rac and UNC-115/AbLIM. *Neuron* 2003;37:53–65. [PubMed: 12526772]
9. Fan X, Labrador JP, Hing H, Bashaw GJ. Slit stimulation recruits Dock and Pak to the roundabout receptor and increases Rac activity to regulate axon repulsion at the CNS midline. *Neuron* 2003;40:113–127. [PubMed: 14527437]
10. Dickson BJ. Rho GTPases in growth cone guidance. *Curr Opin Neurobiol* 2001;11:103–110. [PubMed: 11179879]
11. Krause M, Leslie JD, Stewart M, Lafuente EM, Valderrama F, Jagannathan R, Strasser GA, Rubinson DA, Liu H, Way M, Yaffe MB, Boussiotis VA, Gertler FB. Lamellipodin, an Ena/VASP ligand, is implicated in the regulation of lamellipodial dynamics. *Dev Cell* 2004;7:571–583. [PubMed: 15469845]
12. Kaufmann N, Wills ZP, Van Vactor D. Drosophila Rac1 controls motor axon guidance. *Development* 1998;125:453–461. [PubMed: 9425140]
13. Ng J, Nardine T, Harms M, Tzu J, Goldstein A, Sun Y, Dietzl G, Dickson BJ, Luo L. Rac GTPases control axon growth, guidance and branching. *Nature* 2002;416:442–447. [PubMed: 11919635]
14. Yang L, Bashaw GJ. Son of sevenless directly links the Robo receptor to rac activation to control axon repulsion at the midline. *Neuron* 2006;52:595–607. [PubMed: 17114045]
15. Lafuente EM, van Puijenbroek AA, Krause M, Carman CV, Freeman GJ, Berezovskaya A, Constantine E, Springer TA, Gertler FB, Boussiotis VA. RIAM, an Ena/VASP and Profilin ligand, interacts with Rap1-GTP and mediates Rap1-induced adhesion. *Dev Cell* 2004;7:585–595. [PubMed: 15469846]
16. Kraynov VS, Chamberlain C, Bokoch GM, Schwartz MA, Slabaugh S, Hahn KM. Localized Rac activation dynamics visualized in living cells. *Science* 2000;290:333–337. [PubMed: 11030651]
17. Bourne HR, Sanders DA, McCormick F. The GTPase superfamily: conserved structure and molecular mechanism. *Nature* 1991;349:117–127. [PubMed: 1898771]
18. Reddien PW, Horvitz HR. CED-2/CrkII and CED-10/Rac control phagocytosis and cell migration in *Caenorhabditis elegans*. *Nat Cell Biol* 2000;2:131–136. [PubMed: 10707082]
19. Struckhoff EC, Lundquist EA. The actin-binding protein UNC-115 is an effector of Rac signaling during axon pathfinding in *C. elegans*. *Development* 2003;130:693–704. [PubMed: 12506000]
20. Lucanic M, Kiley M, Ashcroft N, L'Etoile N, Cheng HJ. The *Caenorhabditis elegans* P21-activated kinases are differentially required for UNC-6/netrin-mediated commissural motor axon guidance. *Development* 2006;133:4549–4559. [PubMed: 17050621]
21. Lin CH, Forscher P. Cytoskeletal remodeling during growth cone-target interactions. *J Cell Biol* 1993;121:1369–1383. [PubMed: 8509456]
22. O'Connor TP, Bentley D. Accumulation of actin in subsets of pioneer growth cone filopodia in response to neural and epithelial guidance cues in situ. *J Cell Biol* 1993;123:935–948. [PubMed: 8227150]
23. Sabry JH, O'Connor TP, Evans L, Torioian-Raymond A, Kirschner M, Bentley D. Microtubule behavior during guidance of pioneer neuron growth cones in situ. *J Cell Biol* 1991;115:381–395. [PubMed: 1918146]
24. Williamson T, Gordon-Weeks PR, Schachner M, Taylor J. Microtubule reorganization is obligatory for growth cone turning. *Proc Natl Acad Sci U S A* 1996;93:15221–15226. [PubMed: 8986791]
25. Frost JA, Khokhlatchev A, Stippec S, White MA, Cobb MH. Differential effects of PAK1-activating mutations reveal activity-dependent and -independent effects on cytoskeletal regulation. *J Biol Chem* 1998;273:28191–28198. [PubMed: 9774440]
26. Obermeier A, Ahmed S, Manser E, Yen SC, Hall C, Lim L. PAK promotes morphological changes by acting upstream of Rac. *Embo J* 1998;17:4328–4339. [PubMed: 9687501]
27. Margolis B, Borg JP. Apicobasal polarity complexes. *J Cell Sci* 2005;118:5157–5159. [PubMed: 16280548]
28. Macara IG. Parsing the polarity code. *Nat Rev Mol Cell Biol* 2004;5:220–231. [PubMed: 14991002]
29. Kay AJ, Hunter CP. CDC-42 regulates PAR protein localization and function to control cellular and embryonic polarity in *C. elegans*. *Curr Biol* 2001;11:474–481. [PubMed: 11412996]

30. Kim SK. Cell polarity: new PARTners for Cdc42 and Rac. *Nat Cell Biol* 2000;2:E143–145. [PubMed: 10934484]
31. Quinn CC, Chen E, Kinjo TG, Kelly G, Bell AW, Elliott RC, McPherson PS, Hockfield S. TUC-4b, a novel TUC family variant, regulates neurite outgrowth and associates with vesicles in the growth cone. *J Neurosci* 2003;23:2815–2823. [PubMed: 12684468]

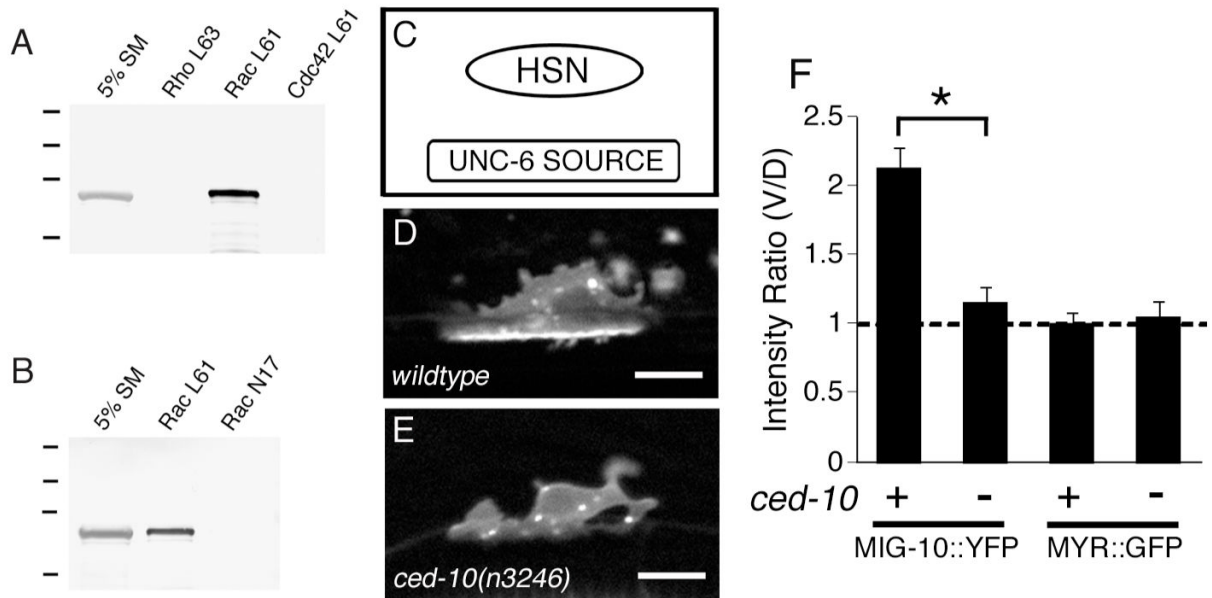


Figure 1.

CED-10/Rac1 binds to MIG-10/lamellipodin and is required for the asymmetric localization of MIG-10/lamellipodin. (A), GST fusion proteins encoding activated mutants of the Rho family GTPases (RhoL63, RacL61, and Cdc42L61) were incubated with the RAPH domain of MIG-10 fused to GFP (MIG-10 RAPH::GFP). MIG-10 RAPH::GFP bound to RacL61 but not Rho L63 or Cdc42L61. (B), MIG-10 RAPH::GFP was incubated with an activated Rac mutant (RacL61) or an inactive Rac mutant (RacN17). MIG-10 RAPH::GFP bound to RacL61 but not RacN17. (C), The UNC-6/netrin guidance cue is expressed from cells located ventral to the HSN and is thought to form a chemotactic gradient that polarizes the HSN [6]. (D), In the wild type background, MIG-10::YFP is localized to the ventral edge of the HSN. Previous work has indicated that this ventral localization is netrin-dependant [6]. (E), In the *ced-10(n3246)* mutant background, MIG-10::YFP fails to localize to the ventral edge of the HSN neuron. (F), Average ventral enrichment of MIG-10::YFP in wildtype (n=12) and *ced-10(n3246)* (n=15) backgrounds. Asterisk indicates $p < 0.0001$ (student's t-test). Myristolated::GFP (MYR::GFP) was not enriched in the wildtype or *ced-10(n3246)* backgrounds. Error bars represent standard error of the mean. Images are of collapsed stacks of optical sections. Ventral is down and anterior is to the left. Scale bars are 5 μ m. The molecular weight markers represent 150, 100, 75 and 50 Kilodaltons.

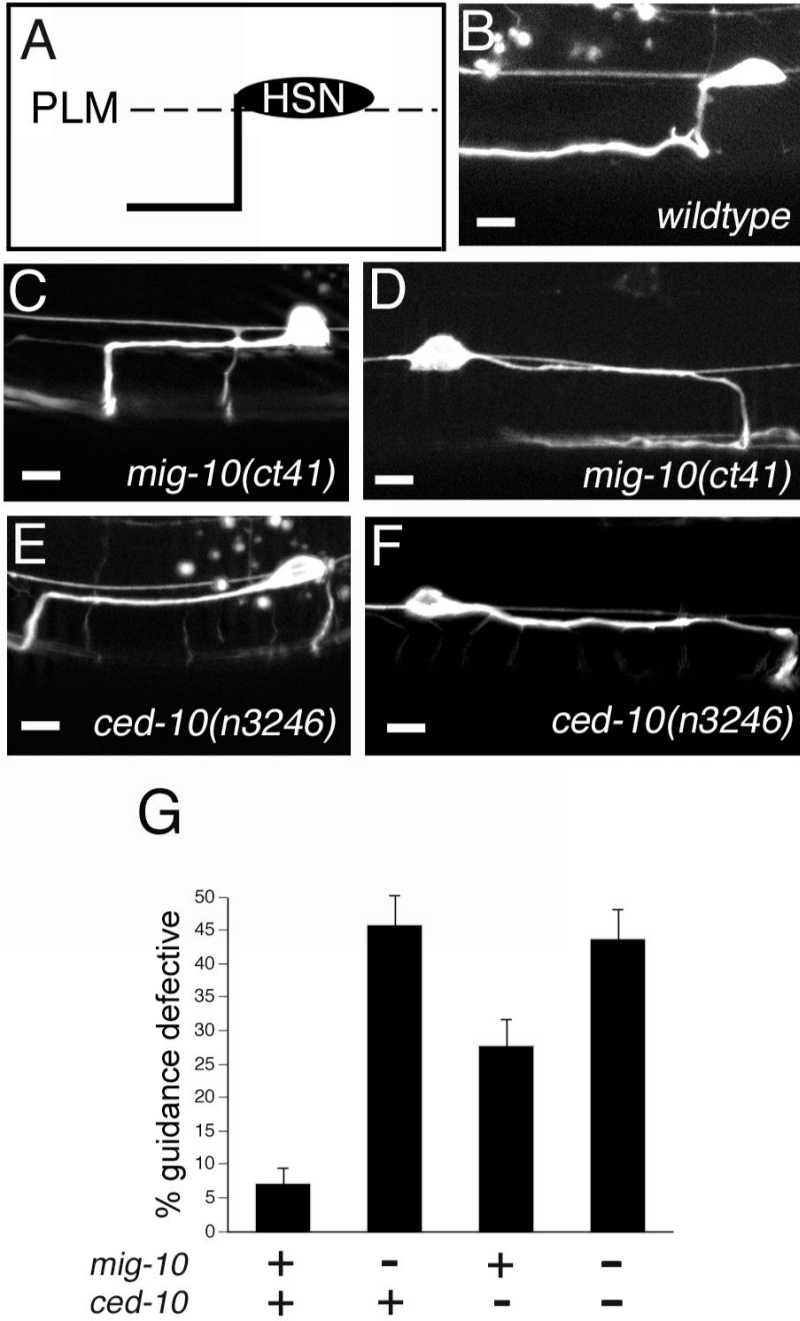
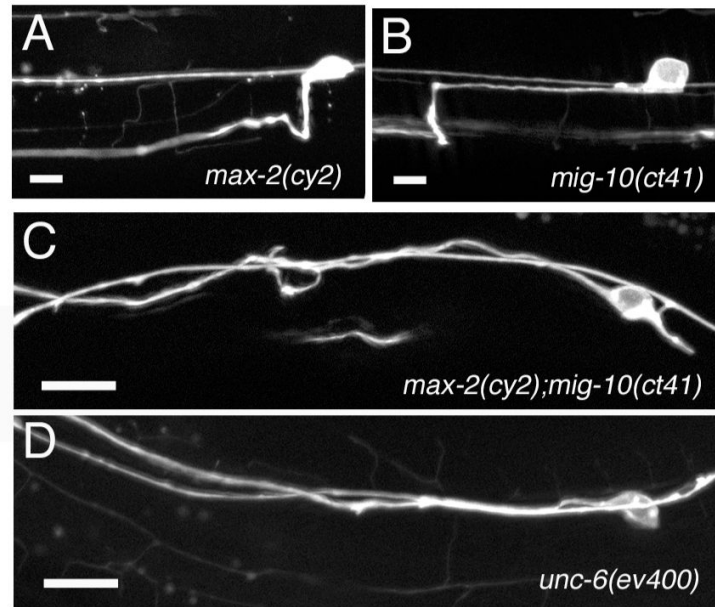


Figure 2. CED-10 functions with MIG-10 to orient HSN axon growth. **(A)** Schematic of normal HSN axon trajectory. The HSN axon makes a ventral migration and then makes an anterior turn to migrate along the ventral nerve cord. **(B)** Example of HSN axon in the wildtype background. **(C and D)** Examples of HSN axon in *mig-10(ct41)* background. In nearly all cases the axon eventually reached the ventral nerve cord. In defective axons, the axon reached the nerve cord after making a lateral migration in the anterior (example shown in c) or posterior (example shown in D) direction. **(E and F)** Similar defects were observed in the *ced-10(n3246)* mutant background. **(G)** Percentage of HSN axons that exhibited guidance defects. The *ced-10;mig-10* double mutant was not enhanced relative to either single mutant. For all

genotypes n=150. Error bars represent standard error of the proportion. Images represent collapsed stacks of optical sections. Ventral is down and anterior is to the left. Scale bars are 5 μm .





E	% mild defect	% severe defect
		
wildtype	7 ±2	0
<i>max-2</i> (-)	6 ±2	0
<i>mig-10</i> (-)	44 ±4	3 ±1
<i>mig-10</i> (-) <i>max-2</i> (-)	13 ±3	57 ±4
<i>pak-1</i> (-)	25 ±4	0
<i>mig-10</i> (-) <i>pak-1</i> (-)	43 ±4	0
<i>unc-6</i> (-)	20 ±3	71 ±4

Figure 3.

MAX-2/PAK-1 functions in parallel to MIG-10/lamellipodin to guide the HSN axon. **(A)** Example of HSN axon in the *max-2(cy2)* null mutant background. Nearly all axons had a normal ventral migration. **(B)** Example of HSN axon in the *mig-10(ct41)* null mutant background. Many of the axons made an abnormal lateral migration prior to making a ventral migration. **(C)** Example of *max-2(cy2); mig-10(ct41)* double null mutant. Many axons failed to make a ventral migration. **(D)** Example of HSN axon in the *unc-6(ev400)* null mutant background. **(E)** Percentage of HSN axons that exhibited mild defects (where the HSN eventually reached the VNC) and percentage of HSN axons that exhibited severe defects (where the HSN never reached the VNC). For all genotypes n=150. Standard error of the

proportion is shown. Images represent collapsed stacks of optical sections. Ventral is down and anterior is to the left. Scale bars are 5 μm .

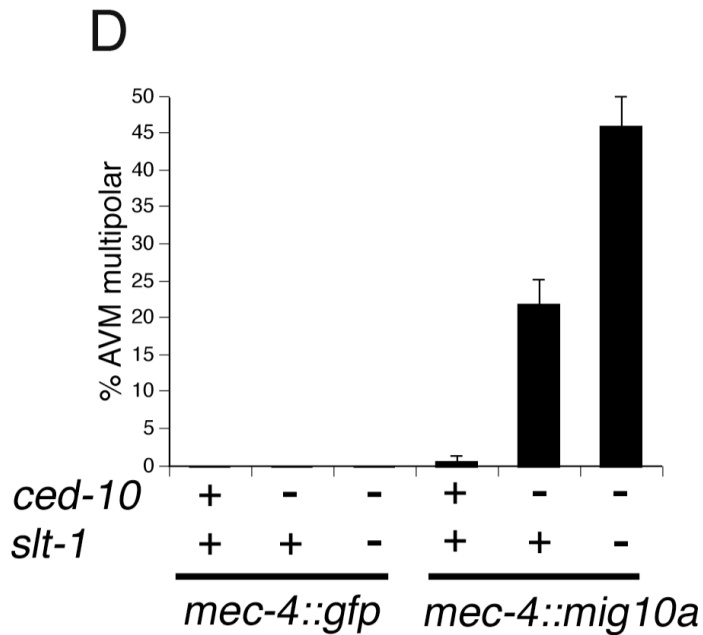
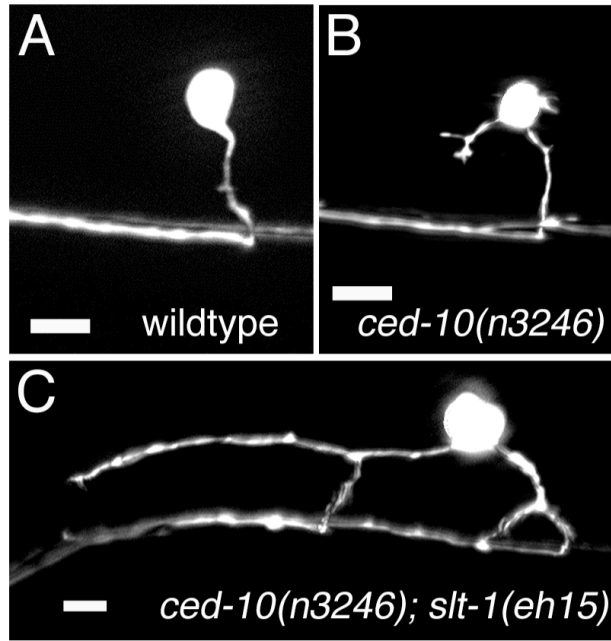


Figure 4. CED-10 is required for the polarization of the MIG-10 outgrowth-promoting activity. **(A)** Example of AVM neuron overexpressing MIG-10A in the wildtype background. **(B)** Example of AVM neuron overexpressing MIG-10A in the *ced-10(n3246)* mutant background. **(C)** Example of neuron overexpressing MIG-10A in the *ced-10(n3246); slt-1(eh15)* double mutant background. **(D)** Percentage of AVM neurons overexpressing GFP or MIG-10A with more than one process growing out of the cell body. The *urEx305* transgene[5], encoding *mec-4::mig-10a*, was used to overexpress MIG-10A in all experiments. For all genotypes n=150. Error bars represent standard error of the proportion. Images represent collapsed stacks of optical sections. Ventral is down and anterior is to the left. Scale bars are 5 μm.

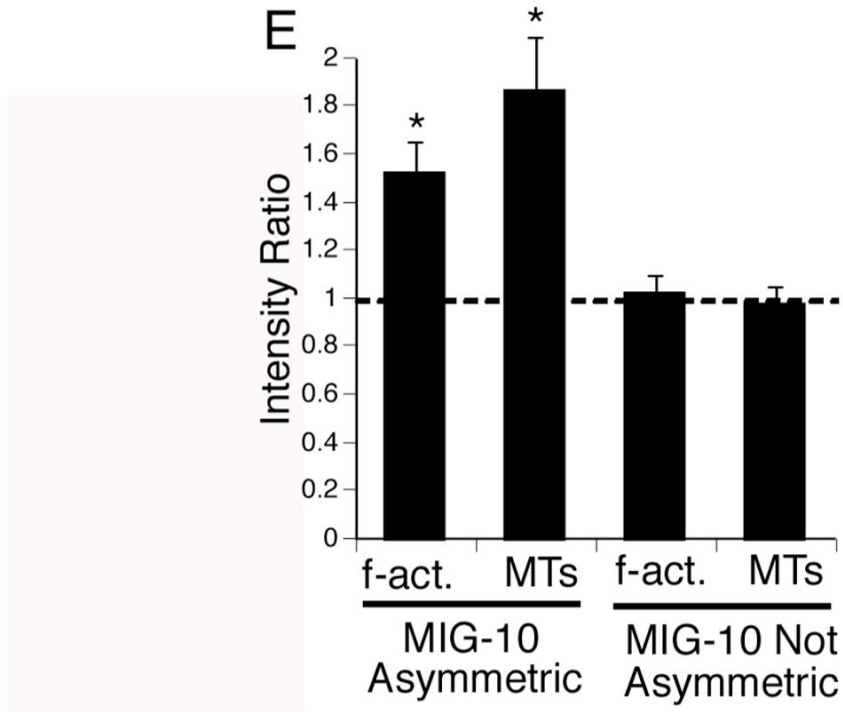
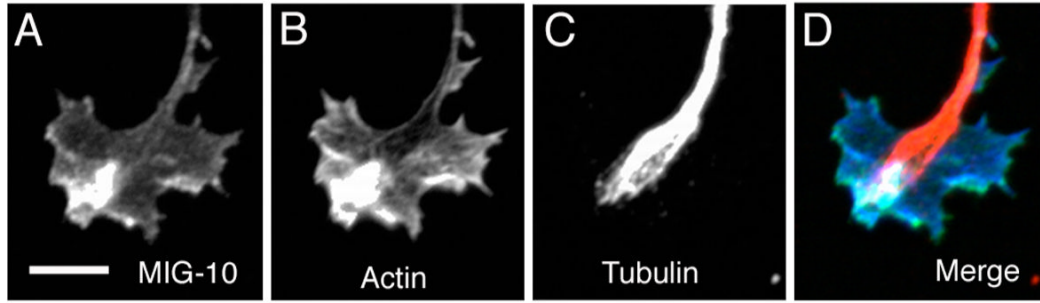


Figure 5. Asymmetric MIG-10 is associated with asymmetric concentrations of f-actin and microtubules in cultured growth cones. **(A-D)** Representative example of a growth cone exhibiting asymmetric concentration of MIG-10::GFP double stained for f-actin and microtubules. **(E)** Analysis of actin and microtubule distribution in growth cones that exhibit asymmetric concentration of MIG-10::GFP (n=6) and growth cones that do not exhibit asymmetric concentration of MIG-10::GFP (n=44). Each growth cone was bisected with a line in parallel to the neurite shaft and the ratio of actin or microtubule fluorescence was calculated. The numerator corresponded to the side of the growth cone with the highest MIG-10 fluorescence. The denominator corresponded to the side of the growth cone with the lowest MIG-10 fluorescence. Asterisk indicates significant difference relative to growth cones without asymmetric MIG-10 (p<0.001, student’s t-test). Error bars represent standard error of the mean. Scale bar is 5 μ m.